The checkerboard pattern of $Bi_{0.63}Sr_{0.37}MnO_3$ determined using resonant x-ray scattering at the Mn K edge

2008 J. Phys.: Condens. Matter 20 235211

(http://iopscience.iop.org/0953-8984/20/23/235211)

J. Phys.: Condens. Matter **20** (2008) 235211 (7pp) doi:10.1088/0953-8984/20/23/235211

The checkerboard pattern of $Bi_{0.63}Sr_{0.37}MnO_3$ determined using resonant x-ray scattering at the Mn K edge

G Subías[1], M C Sánchez[1], J García[1], J Blasco[1], J Herrero-Martín[2], C Mazzoli[2], P Beran[3], M Nevřiva[4] and J L García-Muñoz[3]

[1] Instituto de Ciencia de Materiales de Aragón, Departamento de Física de la Materia Condensada, CSIC-Universidad de Zaragoza, C/Pedro Cerbuna 12, 50009-Zaragoza, Spain
[2] European Synchrotron Radiation Facility, Boite Postal 220, F-38043 Grenoble Cedex, France
[3] Institut de Ciència de Materials de Barcelona, CSIC, Campus Universitari de Bellaterra, E-08193 Bellaterra, Spain
[4] Institute of Chemical Technology, Technická 5, 16628 Prague 6, Czech Republic

Received 28 February 2008, in final form 7 April 2008
Published 6 May 2008
Online at stacks.iop.org/JPhysCM/20/235211

Abstract

A study using resonant x-ray scattering at the Mn K edge has been carried out on a $Bi_{0.63}Sr_{0.37}MnO_3$ single crystal. This compound undergoes a metal–insulator phase transition to the so-called charge ordered (CO) state at about 530 K. Strong resonance signals were observed at room temperature as the energy was tuned through the Mn K edge for several superstructures of the CO phase. The energy, polarization and azimuth angle dependences agree with a checkerboard ordering in the *ab* plane of manganese atoms of two types, in terms of their different local geometrical structures. One of the sites is anisotropic—a tetragonal distorted oxygen octahedron—and the other is isotropic—a nearly undistorted one, as observed for $Bi_{0.5}Sr_{0.5}MnO_3$ and other half-doped manganites. This result indicates that the checkerboard pattern is strongly stable and extends to doping concentrations $x < 0.5$. No superstructures corresponding to the doubling of the *c* axis were detected. Intermediate valence states lower than 3.5, according to the fractional charge segregation, were deduced for the two non-equivalent Mn atoms, i.e. $Mn^{3.30+}$ and $Mn^{3.44+}$.

1. Introduction

For mixed valence metal oxides, the metal–insulator transitions related to charge localization, orbital ordering (OO) or charge ordering (CO) are currently the object of intensive investigations [1–3]. Manganites such as $RE_{1-x}A_xMnO_3$ (RE = trivalent rare earth atom and A = divalent cation) have Mn atoms with a fractional valence state that goes from 3+ to 4+ linearly with the x content. In a purely ionic picture, the formal average valence $Mn^{3.x+}$ is described as formed by $(1-x)Mn^{3+}$ ions plus x Mn^{4+} ions. It was originally thought that, below the metal–insulator transition, Mn^{3+} and Mn^{4+} ions localized at different crystal sites, the so-called CO. Associated with this CO, the occupations of the localized atomic d states (e_g states) are simultaneously ordered, giving rise to the so-called OO physics [4]. In fact, the insulator ordered phase of half-doped manganites ($RE_{0.5}A_{0.5}MnO_3$) is explained as formed by the checkerboard orderings of two different Mn atoms that should be ascribed to Mn^{3+} and Mn^{4+}, respectively [5]. We remember here that the measured charge difference between the two distinct Mn atoms is far from the one-electron segregation [6–9].

Bismuth-based manganites $Bi_{1-x}A_xMnO_3$ (A = Ca, Sr) have recently received great attention because of the occurrence of the metal–insulator transitions well above room temperature for a wide range of A doping [10–17]. Despite the smaller size of Ca compared to Sr, CO is more stable upon heating in $Bi_{0.5}Sr_{0.5}MnO_3$ than in $Bi_{0.5}Ca_{0.5}MnO_3$ [12]. In the (Bi, Sr)MnO_3 system the metal–insulator transition temperature for $x = 0.5$ occurs near 500 K [12] while for the $x = 0.25$ compound it is about 600 K [13, 14][5]. The ordered configuration as a function of the Sr content (x)

[5] We wish to mention here that in [13, 14] there was probably a mistake in the labeling of some electron diffraction peaks (related to a mixing up of *Ibmm* and *Imma* descriptions) which is currently being revised.

is an object of intensive debate. High resolution electron microscopy studies proposed the alternation of double stripes of one sort of Mn^{3+}-like octahedron with double (for $x = 1/3$ and $1/2$) or quadruple (for $x = 2/3$) stripes of a second sort of Mn^{4+}-like octahedron [15, 16]. A double lattice modulation (0 1/2 0) and (0 0 1/2) was reported from electron diffraction (ED) studies on $Bi_{0.75}Sr_{0.25}MnO_3$ and $Bi_{0.67}Sr_{0.33}MnO_3$ with an *Ibmm* average cell [13, 14, 16]. Moreover, a symmetry change of the average cell from *Ibmm*, below T_{CO}, to *Pbnm*, above T_{CO} [13–17], has been observed.

The CO phase transition is usually a structural transition that lowers the symmetry and differentiates between crystallographic transition metal (TM) sites that are equivalent in the high temperature phase. Resonant superlattice reflections appear at the TM K absorption edge due to the differences between the anomalous atomic scattering factors of related atoms in the unit cell [18]. The anomalous atomic scattering factor (ASF) is a symmetric tensor of second rank for dipole transitions. Due to this characteristic, resonant x-ray scattering (RXS) intensity arising from the anomalous part shows azimuth angle and polarization dependence, which is particularly useful for properly characterizing the local symmetry and ordering for different TM sites. Resonance can arise because either TM atoms occupy non-equivalent crystallographic sites and consequently the ASF tensors describing each of the TM atoms are different (CO reflections) or TM atoms occupy equivalent sites but the orientations of the anisotropic ASF tensors are different for distinct TM atoms [19, 20]. These latter reflections are known as anisotropies of the tensor of susceptibility (ATS) reflections. The Thomson scattering is zero for these reflections and they only appear at energies close to the absorption edge. RXS experiments have solved the periodicity of the charge disproportion (so-called CO) and/or anisotropic ordering (so-called OO) in manganites [8, 9, 21–25]. A checkerboard arrangement of two distinct Mn sites in the *ab* plane is found for compositions $x = 0.5$ (half-doped manganites), though the charge disproportion is much smaller than 1 [8, 9, 25].

Bearing in mind that CO for x different from 0.5 is in general not well defined, we have explored further the $Bi_{1-x}Sr_xMnO_3$ system, toward the Mn^{3+}-rich side. We present here a study of the charge and orbital modulation in an off-stoichiometric $Bi_{0.63}Sr_{0.37}MnO_3$ sample using RXS at the Mn K edge[6]. Reflections of the type $(0, k, 0)$, $(0, k/2, 0)$ with $k =$ odd were observed and reflections of the type $(h, k, 1/2)$ were absent. Detailed measurements of the polarization and azimuth angle dependence have been carried out to determine the ordering model. The temperature evolutions of the intensities and wavevector were also studied. The results show that the ordered phase of this bismuth manganite with $x < 0.5$ corresponds to the same checkerboard pattern of two distinct Mn atoms as the $Bi_{0.5}Sr_{0.5}MnO_3$ compound. The important result is that the observed ordering does not match with a 2:1 Mn^{3+}/Mn^{4+} ordering. Furthermore, intermediate valence states lower than 3.5 were deduced for the two distinct Mn atoms.

[6] A summary of this study was presented at the x-ray absorption fine structure (XAFS XIII) conference [26].

2. Experimental method

Crystals of $Bi_{0.63}Sr_{0.37}MnO_3$ were grown by a Bi_2O_3 self-flux method to avoid contamination. The precursors Bi_2O_3, $SrMnO_3$ and MnO_2 were mixed in stoichiometric ratios Bi:Sr:Mn = 67:33:100 and Bi_2O_3 excess (82.5% in weight) was added. The procedure followed was similar to the process used to obtain the $Bi_{0.5}Sr_{0.5}MnO_3$ single crystal studied in [9]. The mixture of precursors and the flux was placed into a 25 cm^3 platinum crucible and preheated at 700 °C for 12 h. The liquid (T_L = 1120 °C) and the eutectic (T_E = 741 °C) temperatures were established. After a period of preheating at $T_L + 50$ K (duration 12 h) the growth process was started at $T_L + 5$ K by decreasing the temperature at a -1 K per hour rate until the temperature $T_E + 50$ K was reached, at which point the furnace was turned off and the solution cooled down to room temperature. The crystal was separated from the flux by heating the mixture in a nitric acid solution; it presented a cubic shape, of 5 mm size. From energy-dispersive analyses, the average composition determined per Mn atom was '$Bi_{0.63(5)}$:$Sr_{0.37(5)}$:Mn_1'. The average structure at RT is described using the orthorhombic *Ibmm* cell with $a = 5.539$ Å, $b = 5.515$ Å and $c = 7.632$ Å. A polished (110) cubic surface was cut for the RXS experiments.

The RXS experiments were carried out at the magnetic scattering undulator beam line ID20 at the European Synchrotron Radiation Facility (ESRF, Grenoble) [27]. The incident beam was monochromatized by double Si(111) crystals located between two focusing mirrors. The energy resolution at the Mn K edge was 1 eV with nearly 100% linear polarization. Polarization analysis of the scattered beam was performed using a Cu(220) crystal analyzer, which gives a scattering angle of 95.9° at the energy of the Mn K edge. The discrepancy from the ideal value of 90° leads to a leakage, estimated at about 2%. The linearly polarized σ' and π' components of the scattered beam are perpendicular and parallel to the diffraction plane, respectively. Rietveld analysis of polycrystalline samples of the composition $Bi_{0.70(4)}Sr_{0.30(4)}MnO_3$ [13, 14] suggested a new type of charge order at RT, characterized by an average *Ibmm* structure ($a_p\sqrt{2} \times a_p\sqrt{2} \times 2a_p$), with a double b and c lattice modulation that produces a larger monoclinic cell. To check this new superstructure, we have recorded both, $(0, k, 0)$ and $(4, 0, l)$ scans, with the incoming beam corresponding to the Mn K absorption edge. Superstructure reflections of the type (0, odd, 0), (0, half-integer, 0), (4, odd, 0), (4, half-integer, 0) and (4, 0, 1) were observed. The energy dependence of the polarized (σ' and π') diffracted intensity was measured through the Mn K absorption edge for these reflections. Azimuthal scans were also performed, rotating the sample by an angle ϕ around the diffraction vector $\mathbf{Q} = \mathbf{k} - \mathbf{k}'$. Around the CO/OO transition temperature of our sample, all the superstructure reflections disappear between 525 and 600 K.

3. Results

3.1. Room temperature results

Figure 1 shows the energy dependence of the (0, 3, 0) reflection for σ–σ' and σ–π' channels at different azimuth angles. The

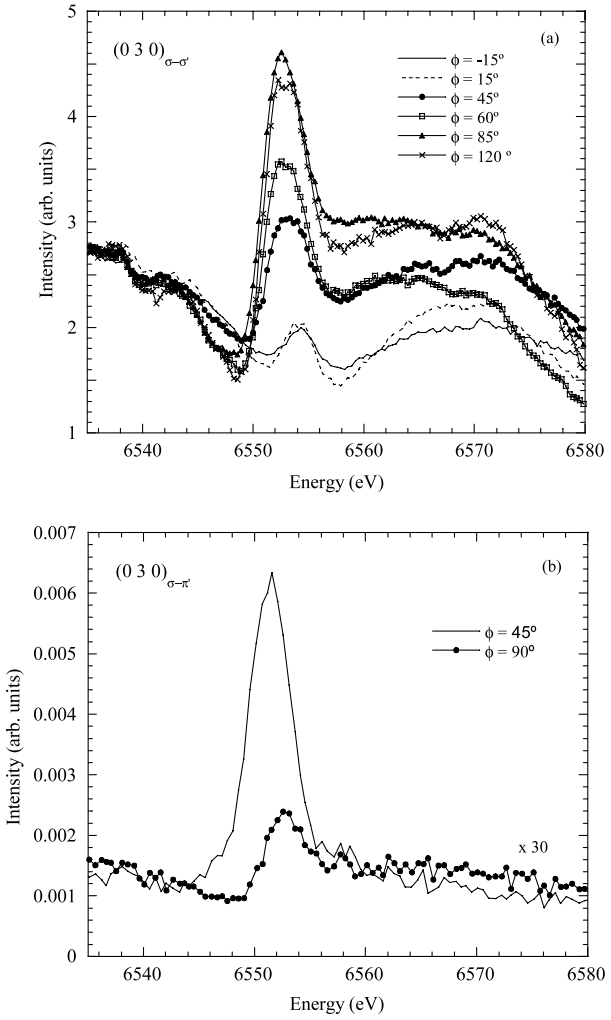

Figure 1. Energy dependence of the intensity of the (0, 3, 0) reflection for σ–σ' (panel (a)) and σ–π' (panel (b)) channels at room temperature and at different azimuth angles ϕ. The azimuth angle $\phi = 0$ corresponds to an incident polarization along the c axis.

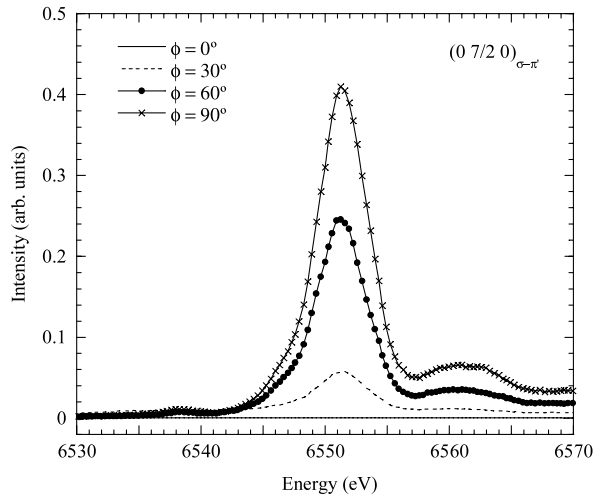

Figure 2. Intensity versus incident photon energy through the Mn K edge of the $(0, 7/2, 0)$ reflection in the σ–π' channel at room temperature.

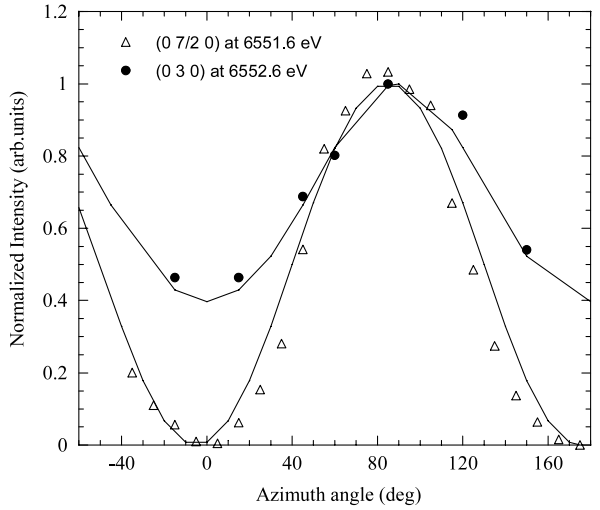

Figure 3. Azimuthal dependence of the $(0, 3, 0)_{\sigma-\sigma'}$ and $(0, 7/2, 0)_{\sigma-\pi'}$ integrated intensities at the energy of the maximum of the resonance at room temperature. Intensities are normalized at the maximum for the sake of comparison. Solid lines are the best-fit curves from the structural checkerboard model.

line shape versus incident photon energy is described as a non-resonant Thomson scattering at energies below the absorption edge and a broad resonance at the Mn K edge. The intensity of the main resonance depends strongly on the azimuth angle. As shown in figure 1, it is maximum for $\phi = 90°$ in the σ–σ' channel and for $\phi = 45°$ in the σ–π' channel. The leakage from the σ–σ' channel was only detected for the $\sigma - \pi'$ channel for $\phi = 90°$. The azimuth angle and the polarization dependence inform us on the anisotropy of the Mn atoms, characteristic of ATS reflections. We have also measured the (0, 5, 0) reflection, which shows an energy dependence and an azimuth evolution similar to those reported for the (0, 3, 0) reflection. These results confirm the dipolar σ–σ' character for (0, odd, 0) reflections.

The energy dependence of the $(0, 7/2, 0)$ reflection across the Mn K edge in the σ–π' channel is shown in figure 2. No intensity was observed in the σ–σ' channel. A large resonance is observed at energies close to the Mn K absorption edge for $(0, 7/2, 0)$ and $(0, 5/2, 0)$ (not reported) reflections. No signal was observed at energies below the absorption edge, showing the absence of Thomson scattering, i.e. these reflections are pure ATS reflections. As shown in figure 2, the intensity of the $(0, 7/2, 0)$ reflection strongly depends on the azimuth angle, but the line shapes are the same for the different ϕ angles.

The azimuth angle dependence of (0, 3, 0) (σ–σ' channel) and $(0, 7/2, 0)$ (σ–π' channel) integrated intensities at the maximum of the resonance peaks are compared in figure 3. The periodicities of each of the reflection types are similar to that found for the $Bi_{0.5}Sr_{0.5}MnO_3$ sample [9], characteristic of the checkerboard ordering model.

We have also looked for other reflections in order to check for the different proposed models. Figure 4 shows the energy dependence for reflections such as $(4, 1/2, 0)$ (4, 1, 0) and (4, 0, 1). The energy dependence of the (4, 1, 0) reflection

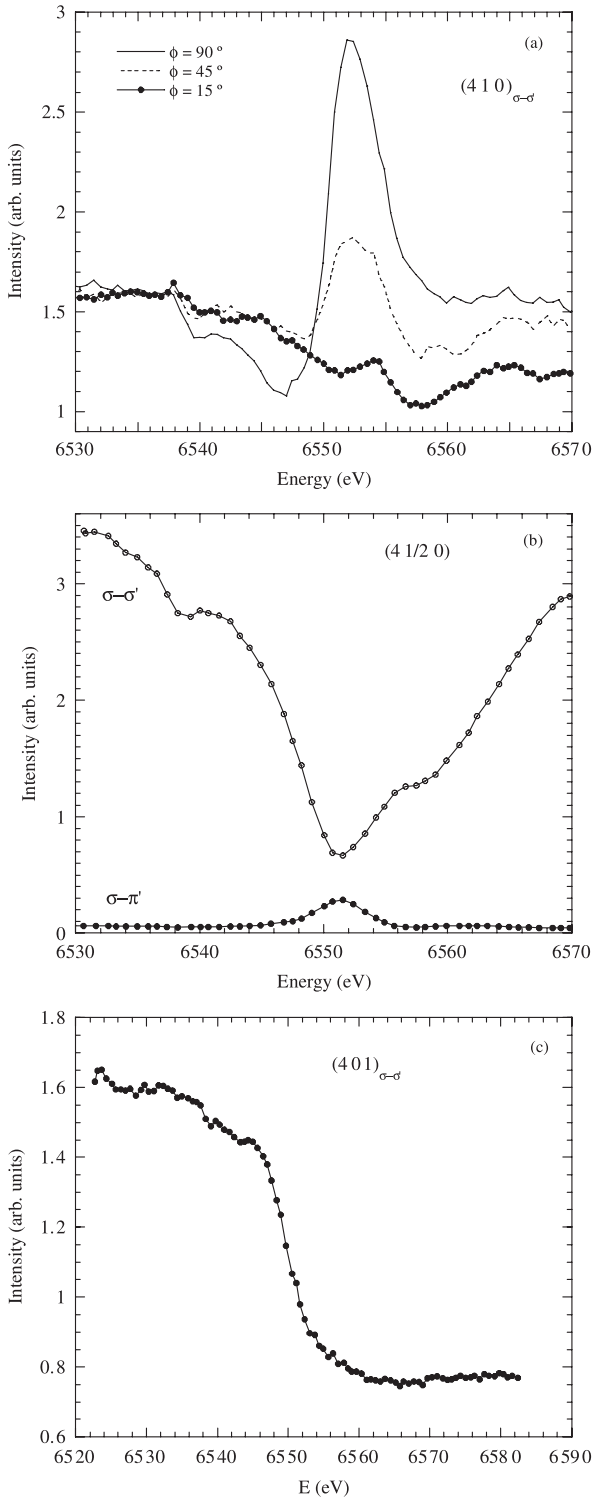

Figure 4. Panel (a): energy dependence of the intensity of the $(4, 1, 0)_{\sigma-\sigma'}$ reflection at different azimuth angles. Panel (b): polarization resolved energy scans of $(4, 1/2, 0)$ reflection taken at the azimuth $\phi = 90°$. Panel (c): energy dependence of the σ–σ' scattered intensity of the (4, 0, 1) reflection. All the energy scans are recorded at room temperature.

is similar to the one observed for (0, 3, 0), as expected, since it will also appear due to the checkerboard ordering. The energy dependence of the $(4, 1/2, 0)$ reflection is the same as that for the $(0, 7/2, 0)$ reflection. However, strong intensity is observed in the σ–σ' channel in this case. As we can see in figure 4, the energy dependence for the σ–σ' channel of the $(4, 1/2, 0)$ reflection shows the usual evolution for anomalous conventional diffraction. This indicates that the σ–σ' intensity is exclusively due to Thomson scattering. So, this periodicity results from the structural modulation due to slight displacement of Mn, Bi(Sr) or oxygen atoms. We note here that these displacements should be transverse to the b axis because of the absence of Thomson scattering for the (0, half-integer, 0) reflections. Finally, some of the proposed models have suggested the doubling of the c lattice parameter [13, 16]. We have carefully checked for reflections of the type (0, 0, half-integer), (odd, 0, half-integer), (even, 0, half-integer) which would show the doubling of the c lattice parameter, but we did not find any of these reflections. We have only observed the (4, 0, 1) in the σ–σ' channel reflection which shows conventional anomalous energy dependence (figure 4(c)). This suggests the lack of any kind of new ordering along the c axis.

3.2. Temperature dependence

Resonant longitudinal scans of the $(0, 3, 0)_{\sigma-\sigma'}$ and $(0, 5/2, 0)_{\sigma-\pi'}$ reflections were measured at different temperatures as shown in figure 5. We observe that the two reflections disappear in the vicinity of T_{CO}, showing that the associated superstructure is characteristic of the so-called CO phase. Despite this general agreement, the two reflections behave differently in the neighborhood of the transition temperature (inset of figure 5(b)). The intensity of the (0, 3, 0) reflection decreases continuously and disappears at about 530 K. In contrast, the $(0, 5/2, 0)$ reflection disappears at the same temperature, but it is substituted by an incommensurate reflection that shifts and widens in the range 525–580 K and, finally, has completely vanished around 593 K. This incommensurate reflection also appears on resonance for the σ–π' polarization channel. Hence, we propose that it could be related to the presence of orbital order small domains, which develop about 50 K above the CO transition temperature.

4. Analysis and discussion

The study performed on different superstructure reflections of the low temperature phase (CO/OO) in $Bi_{0.63}Sr_{0.37}MnO_3$ has allowed us to gain insight into the kind of ordering present in manganites with x different from 0.5. During this study our efforts to detect reflections of the type (h, k, half-integer) were all unsuccessful. Hence, the absence of those reflections leads us to conclude that there is no well-developed 'c' duplication of the cell in this crystal. This result contrasts with previous results which claim c duplication for compounds with $x = 0.25$ and 0.33 [13, 16]. On the other hand, the observation of strong resonance at the Mn K edge in (0, half-integer, 0) and $(4, 1/2, 0)$ reflections demonstrates the duplication of the b unit cell parameter. The polarization and azimuth angle dependences of (0, odd, 0) and (0, half-integer, 0) reflections are equal to those observed for other half-doped manganites such as $Nd_{0.5}Sr_{0.5}MnO_3$ [8] and $Bi_{0.5}Sr_{0.5}MnO_3$ [9] showing

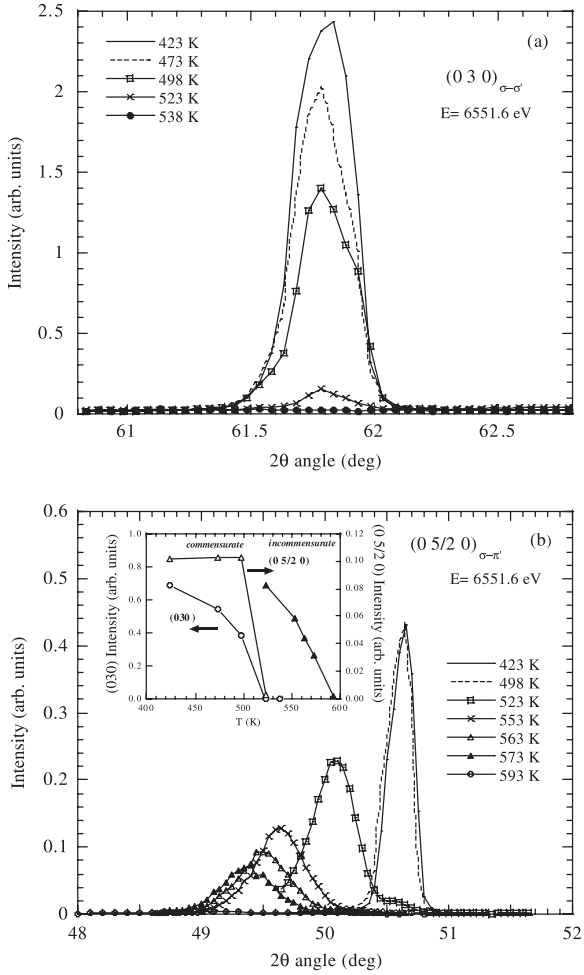

Figure 5. Longitudinal scans of the $(0, 3, 0)_{\sigma-\sigma'}$ (panel (a)) and $(0, 5/2, 0)_{\sigma-\pi'}$ (panel (b)) reflections taken at the energy of the maximum resonance on heating. Inset: integrated intensity for both reflections across the CO transition temperature. Open and solid triangles refer to the commensurate $(0, 5/2, 0)$ and the new incommensurate reflections, respectively.

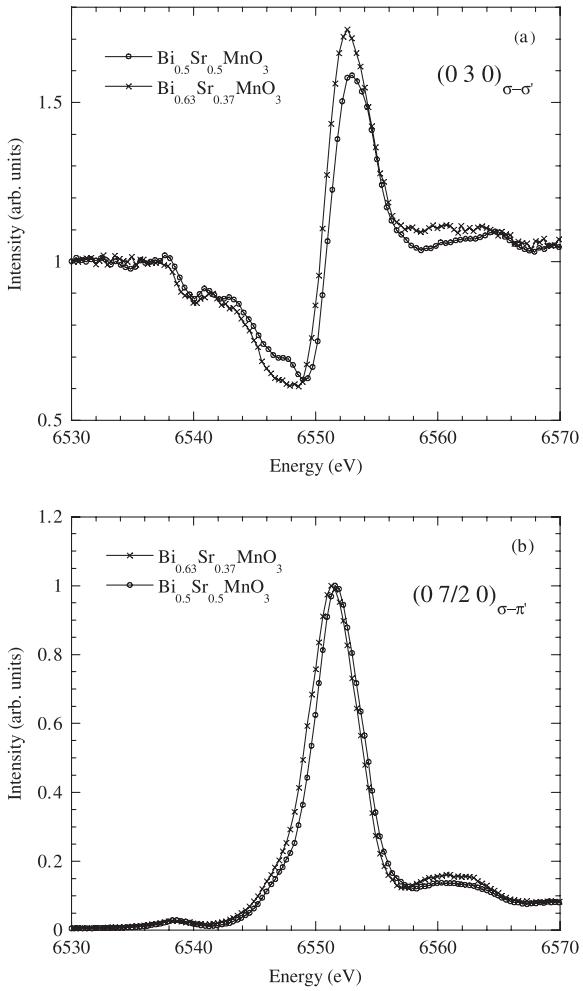

Figure 6. Panel (a): comparison between the RXS intensity of the (0, 3, 0) reflections in $Bi_{0.5}Sr_{0.5}MnO_3$ and that of those in $Bi_{0.63}Sr_{0.37}MnO_3$ at room temperature. Panel (b): comparison between the RXS intensity of the $(0, 7/2, 0)_{\sigma-\pi'}$ reflections in $Bi_{0.5}Sr_{0.5}MnO_3$ and that of those in $Bi_{0.63}Sr_{0.37}MnO_3$ at room temperature.

an equal Mn ordering. For illustration, figure 6 shows the comparison between the energy dependences of the (0, 3, 0) and $(0, 7/2, 0)$ resonant reflections for the samples $Bi_{0.5}Sr_{0.5}MnO_3$ and $Bi_{0.63}Sr_{0.37}MnO_3$. This equivalence also works for the $(4, 1/2, 0)$ reflection, showing that the structural modulation, which duplicates the cell in the b direction, corresponds to small transverse displacements of the atoms in the x direction. This result speaks against the 3:1 ordering of rows of Mn^{3+}-like and Mn^{4+}-like atoms in the ab plane claimed for the $Bi_{0.75}Sr_{0.25}MnO_3$ sample [17]. Therefore, the kind of ordering for $Bi_{0.63}Sr_{0.37}MnO_3$ is a checkerboard pattern of tetragonal anisotropic and nearly isotropic Mn atoms in the ab plane. The possibility of two mixed commensurate phases, one with half-doping and the other with 1/4 doping, is also completely ruled out by the experimental data.

As we have already published a detailed discussion on the analysis of RXS in half-doped compounds, we refer the reader to our published papers [7–9]. The strong similarity of the two samples permits us to extrapolate the quantitative results that we deduce in the analysis of the half-doped bismuthate. As was described in [9], the resonance appears at the absorption edge because the energy dependences of the absorption spectra (the anomalous ASF) of the two kinds of Mn atoms differ due to either different chemical states (valence) or different geometrical anisotropies of the local structures. The azimuth angle and polarization dependences are well described by the checkerboard pattern with an anisotropic Mn atom (uniaxial anisotropy) and an isotropic Mn atom. We summarize here the polarization and azimuth angle dependences of the scattered intensities for (0, odd, 0) and (0, half-integer, 0) reflections, which completely agree with the experimental evolution:

$$I_{\sigma-\sigma'}(0k0) = [C_k + 2(f_\perp - f)\cos^2\phi + (f_\parallel + f_\perp - 2f)\sin^2\phi]^2$$

$$I_{\sigma-\pi'}(0k0) = [(f_\perp - f_\parallel)\sin\phi\cos\phi\sin\theta]^2$$

$$I_{\sigma-\sigma'}(0k/20) = 0$$

$$I_{\sigma-\pi'}(0k/20) = [(f_\parallel - f_\perp)\sin\phi\cos\theta]^2.$$

Here C_k is the Thomson contribution, $f_\parallel$ and $f_\perp$ are the parallel and perpendicular components of the ASF of the anisotropic Mn atom and f is the ASF of the undistorted Mn atom, ϕ and θ are the azimuth and scattering angles, respectively. As has been discussed in [8, 9], other ordering models such as double stripes and Zener polaron [28] ones do not reproduce the observed polarization and azimuth angle dependences.

We used a semi-empirical model that accounts for the energy dependence of the resonant scattering for either (0, odd, 0) or (0, half-integer, 0) reflections, as was done in [8, 9]. An experimental fluorescence spectrum was used to extract the imaginary part f'' of the anomalous correction ($f(E) = f'(E) + \mathrm{i}f''(E)$), and the real part f' is calculated through Kramers–Kronig transformation of f'' [29]. The different diagonal f components of the two different Mn atoms are then deduced from overall energy shifts of the absorption edge, assuming no significant change in the near-edge structure. These are the chemical shift ($\delta_{\mathrm{chemical}}$), which measures the different charges on the Mn atoms, and the anisotropic shift ($\delta_{\mathrm{anisotropic}}$), which is a measure of the local tetragonal distortion. As is shown in figure 6, the resonances observed for the two samples are nearly identical, indicating the same $\delta_{\mathrm{anisotropic}}$ and $\delta_{\mathrm{chemical}}$ parameters. Therefore, we can conclude that the charge disproportion and the tetragonal distortion must be nearly equal for the two samples. We recall here that the charge disproportion for half-doped bismuthate was $\delta = 0.14 \pm 0.05$ electrons [9]. Assuming an equal disproportion, the valence of the isotropic Mn atom should be $Mn^{3.44+}$ and for the anisotropic one[7], $Mn^{3.30+}$. We can note in figure 6 that there is a slight energy shift between the two resonances. This energy shift agrees with the chemical shift between the absorption spectra and comes from the different averaged valences of the Mn atom. The formal valence state for $x = 0.37$ is 3.37+ whereas it is 3.5+ for the $x = 0.5$ sample, in agreement with a shift of the absorption edge to higher energies in the latter.

It is believed that the ground state for the composition $x = 0.25$ (and 0.33), on one hand, and $x = 0.50$, on the other hand, is formed by two different charge and orbital ordered configurations. The first (apparently doubly modulated) occurs with a typical transition temperature of 600 K, and the second (single modulation) takes place around 500 K. We have determined our single crystal to be $Bi_{0.63}Sr_{0.37}MnO_3$. Several issues need to be emphasized. (I) The composition of our crystal is exactly at the halfway point along the distance that separates $x = 0.25$ and 0.50 compositions. (II) We have not observed the second modulation ((0 0 1/2) referred to $Ibmm$) previously reported for $Bi_{1-x}Sr_xMnO_3$ samples with $x = 0.25$–0.33. (III) Our RXS results agree with a checkerboard ordering in the ab plane of manganese atoms of two types with different local geometrical structures, as reported for $Bi_{0.50}Sr_{0.50}MnO_3$. (IV) The transition temperature is more similar to that of the $Bi_{0.75}Sr_{0.25}MnO_3$ system, and clearly higher than for $Bi_{0.50}Sr_{0.50}MnO_3$ (see the inset of figure 5 compared with figure 2 in [9]). After all these considerations we are led to the conclusion that there is no direct relationship between the appearance of the second modulation in the ordered structure and the augmentation of the transition temperature from 500 to 600 K.

Another important point to be stressed is that the ordering of the $Bi_{0.63}Sr_{0.37}MnO_3$ sample does not match with a distribution of formal Mn^{3+} and Mn^{4+} ions according to the chemical composition x. The ratio between Mn^{3+} and Mn^{4+} ions should be larger than 1 (to be exact, $63/37 = 1.70$), which contrasts with the 1:1 proportion between the two kinds of manganese atoms resulting from the checkerboard ordering. This result also contrasts with the structural determination of the close sample $Bi_{0.75}Sr_{0.25}MnO_3$, which obtains three different valence states for the four Mn sites, indicating then a 3:1 Mn^{3+}/Mn^{4+} charge ordering [17]. The formation of a checkerboard ordering when the formal Mn^{3+}/Mn^{4+} ratio is different from 1:1 has also been observed for $Pr_{0.6}Ca_{0.4}MnO_3$ [23, 25]. These two experimental evidences seem to indicate strong stability of the checkerboard ordering in manganites. On the other hand, we would like to note that for $x > 0.5$, several experiments have probed whether the ordering agrees with the formal Mn^{3+}/Mn^{4+} relationship [30] despite the charges on the Mn atoms being far from the ionic ones. This strong dissymmetry as regards the kind of order of the CO phase as a function of the doping is a matter for further detailed studies. Moreover, a common feature of all the mixed valence TM oxides is that the charge segregation is always very small and very far from an ionic description. A recent experiment on $Bi_{0.5}Sr_{0.4}Ca_{0.1}MnO_3$ by scanning transmission electron microscopy corroborates this fact, as no periodic valence modulation between the two sorts of Mn atoms was observed in the so-called CO phase [31]. Therefore, the electronic localization responsible for the metal–insulator phase transition would occur in clusters involving several TM atoms instead of on an atomic level.

We will also note that the appearance of an incommensurate $(0, 5/2 - \delta, 0)$ reflection in a temperature range of 50 K above T_{CO} suggests a strong correlation between anisotropic Mn atoms. This observation can be explained by the existence of dynamical local distortions above T_{CO}, which are highly correlated near T_{CO} and freeze in an ordered pattern of distortions below the transition temperature. This mechanism was already proposed for the M–I phase transition in $LaMnO_3$ where the local atomic arrangement of the Mn atoms is dynamically distorted above the so-called Jahn–Teller phase transition temperature [32].

Summarizing, the CO–OO phase in the low doping regime of $Bi_{1-x}Sr_xMnO_3$ perovskites mainly results from the structural modulation, which differentiates between two Mn sites that were crystallographically equivalent above T_{CO} with very small associated valence modulation.

Acknowledgments

This work was financially supported by the Spanish CICyT Grants No. MAT2005-04562 and MAT2006-11080-C02-02 projects, the Diputación General de Aragón (DGA-CAMRADS, PIPO18/2005), and the Generalitat de Catalunya

[7] We note here that the ascribed valence is formal. It is assumed that the charges of the Mn atoms in $BiMnO_3$ and $SrMnO_3$ are Mn^{3+} and Mn^{4+} respectively. Therefore, the intermediate valence $Mn^{3.x+}$ means that the charge on the Mn atom is that of the $BiMnO_3$ reference sample plus x times the charge difference between the Mn atoms in $BiMnO_3$ and $SrMnO_3$.

(2005-GRQ-00509). The FAME European Network of Excellence is also acknowledged. The authors thank ESRF for granting beam time.

References

[1] Tsuda N, Nasu K, Yanase A and Siratori K 1990 *Electronic Conduction in Oxides* (Berlin: Springer)
[2] Daggoto E, Hotta T and Moreo A 2001 *Phys. Rep.* **344** 362
[3] García J and Subías G 2004 *J. Phys.: Condens. Matter* **16** R145
[4] Goodenough J B 1955 *Phys. Rev.* **100** 564
[5] Radaelli P G, Cox D E, Marezio M and Cheong S-W 1997 *Phys. Rev.* B **55** 3015
[6] Subías G, García J, Proietti M G and Blasco J 1997 *Phys. Rev.* B **56** 8183
[7] Garcia J, Sánchez M C, Subías G and Blasco J 2001 *J. Phys.: Condens. Matter* **13** 3243
[8] Herrero-Martin J, García J, Subías G, Blasco J and Sánchez M C 2004 *Phys. Rev.* B **70** 024408
[9] Subías G, García J, Beran P, Nevriva M, Sánchez M C and García-Muñoz J L 2006 *Phys. Rev.* B **73** 205107
[10] Bokov V A, Grigorya N A and Bryzhina M F 1967 *Phys. Status Solidi* **20** 745
[11] Gupta A, Samanta S B, Awana V P S, Kishan H, Awasthi A M, Bhardwaj S, Narlikar A V, Frontera C and García-Muñoz J L 2005 *Physica* B **370** 172
[12] García-Munoz J L, Frontera C, Llobet A and Ritter C 2001 *Phys. Rev.* B **63** 064415
[13] Frontera C, García-Muñoz J L, Aranda M A G, Hervieu M, Ritter C, Mañosa L, Capdevila X G and Calleja A 2003 *Phys. Rev.* B **68** 134408
García-Muñoz J L *et al* 2003 *J. Solid State Chem.* **171** 84
[14] García-Muñoz J L, Frontera C, Raspaud M, Giot M, Ritter C and Capdevila X G 2005 *Phys. Rev.* B **72** 054432
[15] Hervieu M, Maignan A, Martin C, Nguyen N and Raveau B 2001 *Chem. Mater.* **13** 1356
[16] Hervieu M, Malo S, Pérez O, Beran P, Martin C, Bladinozzi G and Raveau B 2003 *Chem. Mater.* **15** 523
[17] Goff R J and Attfield J P 2006 *J. Solid State Chem.* **179** 1348
[18] Materlik G, Sparks C J and Fisher H 1994 *Resonant Anomalous X-ray Scattering: Theory and Applications* (Amsterdam: Elsevier/North-Holland)
[19] Templeton D H and Templeton L K 1980 *Acta Crystallogr.* **36** 237
[20] Dmitrienko V E, Ishida K, Kirfel A and Ovchinnikova E N 2005 *Acta Crystallogr.* A **61** 481 and references therein
[21] Murakami Y, Kawada H, Tanaka M, Arima T, Moritomo Y and Tokura Y 1998 *Phys. Rev. Lett.* **80** 1932
[22] Murakami Y *et al* 1998 *Phys. Rev. Lett.* **81** 582
[23] Zimmerman M V *et al* 2001 *Phys. Rev.* B **64** 195133
[24] Subías G, Herrero-Martin J, García J, Blasco J, Mazzoli C, Hatada K, di Mateo S and Natoli C R 2007 *Phys. Rev.* B **75** 23501
[25] Grenier S *et al* 2004 *Phys. Rev.* B **70** 134419
[26] Hedman B and Pianetta P (ed) 2007 *XAFS XIII: X-ray Absorption Fine Structure* p 361 AIP CP882
[27] Paolasini L *et al* 2007 *J. Synchrotron Radiat.* **14** 301
[28] Daoud-Aladine A, Rodriguez-Carvajal J, Pinsard-Guadard L, Fernandez-Diaz M T and Revcolevski A 2002 *Phys. Rev. Lett.* **89** 097205
[29] Cromer D T and Liberman D 1970 *J. Chem. Phys.* **53** 1891
[30] Larochelle S, Mehta A, Lu L, Mang P K, Vajk O P, Kaneko N, Lynn J W, Zhou L and Greven M 2005 *Phys. Rev.* B **71** 024435
[31] Loudon J C, Fitting Kourkoutis L, Ahn J S, Zhang C L, Cheong S-W and Muller D A 2007 *Phys. Rev. Lett.* **99** 237205
[32] Sánchez M C, Subías G, García J and Blasco J 2003 *Phys. Rev. Lett.* **90** 045503